Direct-Coupled TE–TM Waveguide Cavities

Simone Bastioli, *Senior Member, IEEE*, Richard Snyder, *Life Fellow, IEEE*,
Cristiano Tomassoni, *Senior Member, IEEE*, and Valentin de la Rubia

***Abstract*— This letter presents a novel structure where TE_{10} and TM_{11} waveguide sections are directly coupled along an inline configuration. Specifically, the basic configuration here reported consists of TE–TM–TE three sections that generate third-order filtering functions having one transmission zero. No dedicated coupling discontinuities (such as irises or slots) are included at the TE–TM interfaces. Hence, due to the higher impedance that the larger TM_{11} section shows at one end of the smaller TE_{10} sections, TE modes resonating with a quarter-wavelength variation along the longitudinal direction become feasible. The adjustment over position and orientation of the TE sections allows to achieve a vast range of independent coupling coefficients, thus guaranteeing some of the largest design flexibility in terms of achievable bandwidths and full control of the transmission zero location. The experimental results of a three-section prototype validate the proposed concept while paving the way for the introduction of an innovative class of direct-coupled TE–TM waveguide filters.**

***Index Terms*— Cavity resonators, direct-coupled filters, elliptic filters, nonresonating modes, waveguides.**

I. Introduction

DUE to their superior performance over any other technology, waveguide filters continue to be a major research topic for microwave engineers [1]. Size saving continues to be one of the most important research goals, especially in the lower portion of the microwave spectrum where waveguide structures become inevitably bulky.

The most efficient way to reduce the size of a conventional waveguide filter without degrading its performance consists of using multiple resonant and/or nonresonating modes, thus obtaining extended capabilities (multiple poles and/or transmission zeros) for each individual cavity. Among the various contributions regarding nonresonating modes, the TM filter concept introduced in [2] can be considered as one of the most important pioneering works. In [2], TM cavities and coupling slots are arranged in such a way so as to generate a pole-zero pair for each individual cavity. The main limitation of these TM filters regards the maximum achievable bandwidth. In truth, bandwidth limitation and/or loss of design flexibility as the required passband increases are issues that significantly affect most of the main contributions involving cavities with extended capabilities [3], [4], [5], [6], [7], [8]. A very interesting technique capable to obtain extremely wide bandwidths is reported in [9], where resonant capacitive irises are employed between TM cavities. Such a filter class is, however, devoted to the realization of quasi-high-pass filters (transmission zeros located below the passband and no defined upper stopband characteristic within the unimodal frequency range). Recently, another couple of interesting contributions focusing on wideband bandpass filters have been reported in [10] and [11], where resonant coupling slots are employed in combination with dual- or single-mode TM cavities. The effectiveness of resonant coupling elements for the realization of wideband or even dual-band filters has also been recently demonstrated in [12]. As is for any structure utilizing resonant coupling elements (including [9]), besides the advantages of increasing the order and the bandwidth of the filter (which was indeed the main objective of Bartlett et al. [10], [11]), limitations commonly arise from the inevitable need to dimension those elements for both resonance and coupling reasons; specifically, the height (and sometimes the length) of each resonant slot is a crucial design and optimization parameter, which controls certain coupling coefficients. Typically, resonant slots/irises having small (or considerably reduced) heights are needed, thus significantly affecting their Q-factor while limiting the power handling of the entire filter.

In this letter, we are introducing a novel structure that can potentially lead to the definition of a more general class of nonresonating mode filters that is able to maintain maximum design flexibility for both very narrow and very wide bandpass responses. The key feature of the new structure is that TE_{10} and TM_{11} waveguide sections are directly coupled to each other without any coupling discontinuity between them. Large ranges of independent coupling coefficients can be achieved by simply controlling the location of the sections at the TE–TM interfaces. In contrast with the usage of resonant coupling elements, the cross section of the TE sections is not obliged to any coupling constraint, and it can therefore be dimensioned as a full-size rectangular waveguide (thus not being subject to the typical Q-factor and power handling reductions that affect reduced-height resonant irises/slots). To prove the proposed concept, a basic TE–TM–TE three-section configuration is going to be discussed and experimentally validated in this letter.

II. TE–TM–TE Three-Section Configuration

The structure of the proposed TE–TM–TE three-section configuration is shown in Fig. 1. The feeding input and output waveguides (source and load) are coupled to the first and last rectangular TE_{10} sections by means of regular inductive irises. The TE_{10} sections are then directly coupled to a square TM_{11} section, the latter serving as a TM_{110} mode cavity. Besides the

Manuscript received 20 February 2023; revised 29 March 2023; accepted 29 March 2023. This article was presented at the IEEE MTT-S International Microwave Symposium (IMS 2023), San Diego, CA, USA, June 11–16, 2023. *(Corresponding author: Simone Bastioli.)*

Simone Bastioli and Richard Snyder are with RS Microwave Company, Butler, NJ 07405 USA (e-mail: sbastioli@rsmicro.com; r.snyder@ieee.org).

Cristiano Tomassoni is with the Department of Engineering, University of Perugia, 06100 Perugia, Italy (e-mail: cristiano.tomassoni@unipg.it).

Valentin de la Rubia is with the Departamento de Matemática Aplicada a las TIC, ETSI de Telecomunicación, Universidad Politécnica de Madrid, 28040 Madrid, Spain (e-mail: valentin.delarubia@upm.es).

Color versions of one or more figures in this letter are available at https://doi.org/10.1109/LMWT.2023.3263905.

Digital Object Identifier 10.1109/LMWT.2023.3263905

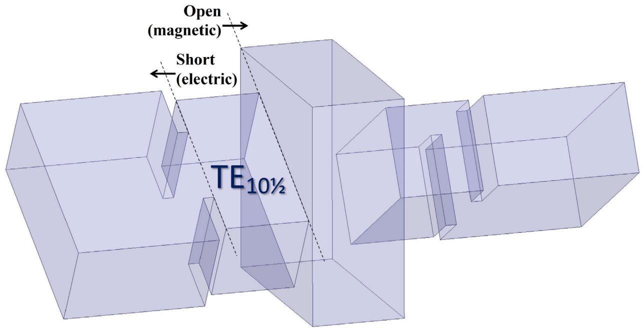

Fig. 1. TE–TM–TE three-section configuration.

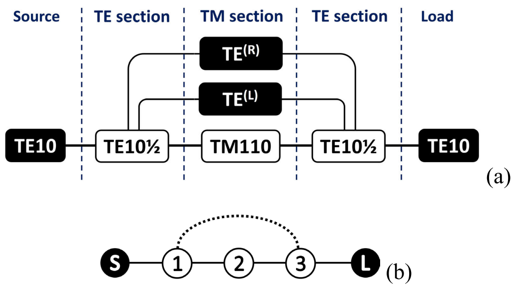

Fig. 2. (a) Modal coupling scheme. (b) Circuit topology. White-filled modes and nodes represent resonant modes and resonators, respectively.

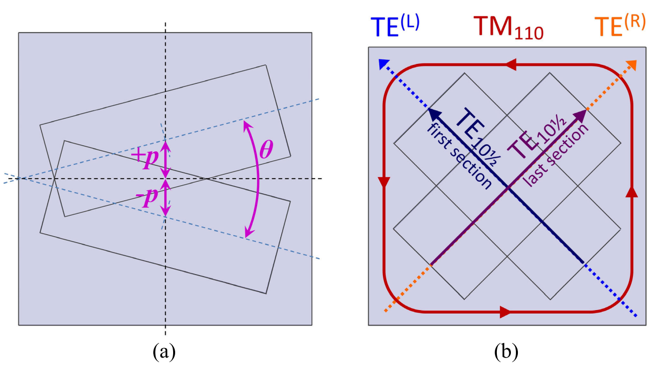

Fig. 3. Longitudinal view of the structure. (a) Coupling control through offset p and angle θ. (b) Structural condition of isolation ($p = 0$ and $\theta = 90°$) and magnetic fields of the involved modes.

resonant TM_{110} mode, the square TM section supports a pair of orthogonal TE modes that are polarized along its diagonals (referred to as diagonal modes $TE^{(L)}$ and $TE^{(R)}$). Since the length of the TM section is around a quarter wavelength, then the diagonal modes behave as nonresonating modes that can provide a bypass coupling between the two TE sections.

As the rectangular TE sections are directly terminated into the much larger square TM section, the equivalent of an open-ended (magnetic) condition is seen at one end of both TE sections. Hence, a TE half-mode resonating with a quarter-wavelength variation along the longitudinal direction becomes feasible within each TE section, with such a half-mode referred to as $TE_{101/2}$.

The coupling and routing scheme between the various modes as well as the equivalent circuit filter topology are shown in Fig. 2(a) and (b), respectively. The resulting triplet topology allows for third-order filtering functions having an independently located transmission zero.

Position and orientation of the TE sections with respect to the TM section are exploited as shown in Fig. 3(a) to

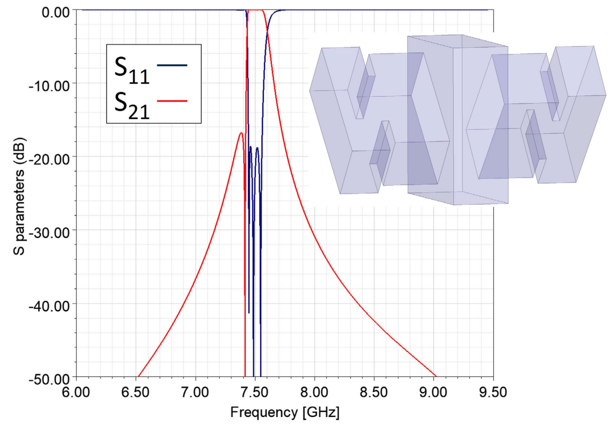

Fig. 4. Full-wave simulation (HFSS) of an optimized 100-MHz bandwidth three-section configuration having a transmission zero in the lower stopband.

fully control all the coupling mechanisms occurring between the various modes. Observe that the cross-sectional size of the TE sections is not employed at all for any coupling purposes and in principle can remain equal to the full size of the standard rectangular waveguide (thus maximizing the unloaded Q-factor of the resonant mode).

Let us consider the structural condition shown in Fig. 3(b) where both TE sections are centered with respect to the square TM section, while each is parallel with one of the two square diagonals ($p = 0$ and $\theta = 90°$). Such a condition results in a total input-to-output isolation. Specifically, due to symmetry reasons, the TM_{110} mode in the square TM section cannot be excited as long as the TE sections are centered ($M_{12} = M_{23} = 0$); moreover, since each TE section is fully parallel with each of the two orthogonal diagonal modes, no bypass coupling can occur ($M_{13} = 0$). Such a condition can be a useful starting point to dimension the structure so that all resonant modes resonate around the desired frequency; to this purpose, the lengths of the TE sections control the resonant frequency of the $TE_{101/2}$ modes, while the side of the square TM section determines the frequency of the TM_{110} mode.

When the TE sections are offset along the vertical direction of the TM cavity, a direct TE–TM coupling (M_{12} and M_{23}) can readily be established: the larger the offset p, the larger the resulting coupling. For the stand-alone three-section structure presented in this letter, the offsets of the first and last TE sections have always the same extent p. Independently of the offset p, however, a bypass coupling can be established only by changing the orientation of the TE sections: as the angle θ between these becomes smaller than 90° (by progressively aligning both TE sections with the horizontal plane), the magnitude of the bypass coupling (M_{13}) increases. As far as the sign of the bypass coupling is concerned, when the TE sections are offset toward opposite directions ($+p$ and $-p$, as is in Fig. 4), a positive sign for M_{13} can be used to reflect the fact that the transmission zero is located above the passband; on the other hand, if the TE sections are offset toward the same direction, the equivalent sign of the bypass coupling M_{13} is negative (transmission zero located below the passband).

Very narrow responses can easily be designed by applying modest deviations (small offsets and limited angle variations) from the starting isolation condition. As the deviations increase, since no coupling discontinuities are present and the cross section of the TE sections is essentially full sized,

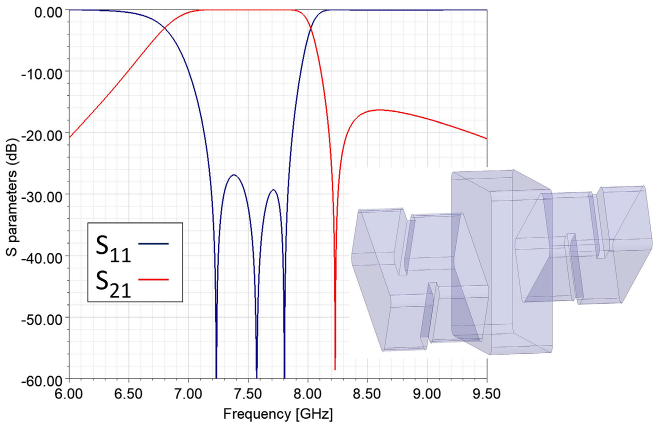

Fig. 5. Full-wave simulation (HFSS) of an optimized 700-MHz bandwidth three-section configuration having a transmission zero in the upper stopband.

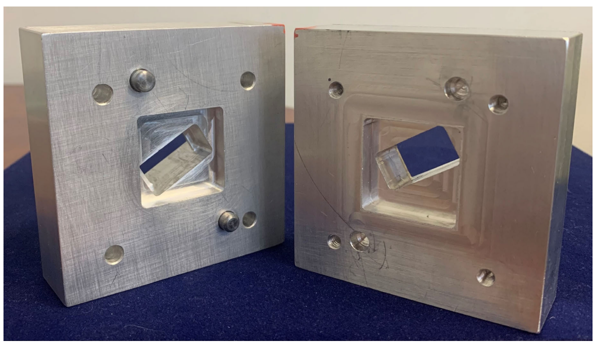

Fig. 6. Manufactured prototype composed of two CNC machined aluminum blocks (WR-112 mounting flanges are realized on the other side of each block).

the coupling coefficients can readily achieve extremely large values, thus easily obtaining very wide bandpass responses.

As the first example, Fig. 4 shows the full-wave simulation (ANSYS HFSS) of a TE–TM–TE three-section configuration with a narrow 100-MHz passband at 7.5 GHz (1.33% fractional bandwidth) and with a lower stopband transmission zero. In order to show the inherent design flexibility of the proposed structure, a second three-section configuration has been optimized at the same frequency for a much wider 700-MHz passband (9.33% fractional bandwidth) and with a transmission zero in the upper stopband. The full-wave simulation of this second structure is shown in Fig. 5.

In our experience, responses having 15% bandwidths while maintaining full control of the zero location are easily achievable with a TE–TM–TE three-section configuration, while even significantly larger bandwidths can be obtained if the position of the zero remains not too far from the passband.

III. Results

The 700-MHz bandwidth structure simulated in Fig. 5 has been manufactured and experimentally validated. A photograph of the manufactured prototype is shown in Fig. 6. Input–output interfaces are standard WR-112. The width of the input–output iris is 18.6 mm (the thickness is 1.52 mm). The width of the TE sections is 24.5 mm, while their length is 9.35 mm. The side of the TM section is 29.22 mm, while its length is 11.5 mm. With reference to Fig. 3, $\theta = 60°$ and $p = 2.5$ mm.

The experimental results are shown in Fig. 7 (Agilent PNA E8362A and Hewlett Packard WR-112 calibration kit). No tuning elements are included in this proof-of-concept computer numerical control (CNC) machined prototype. The measured insertion loss is around 0.04 dB, thus revealing an average experimental Q-factor of around 5600 for the three resonant modes (the simulated unloaded Q-factors considering ideal silver surfaces are 8000 for the $TE_{101/2}$ modes and 9300 for the TM_{110} mode).

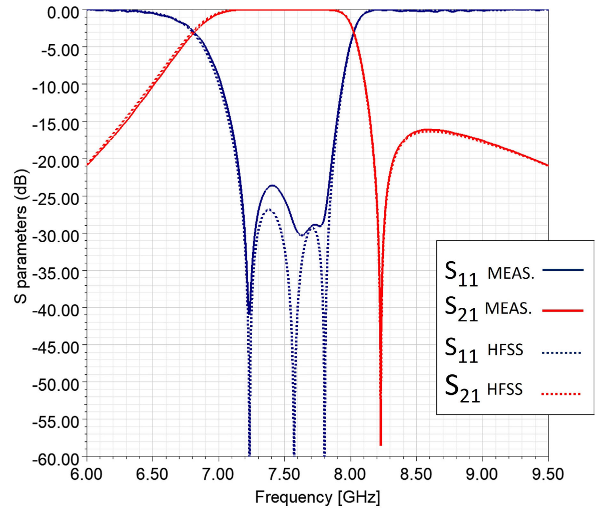

Fig. 7. Experimental results: measured versus simulated S-parameters.

Observe that although no postfabrication tuning has been necessary for this relatively wideband and low-order prototype, it is expected that some sort of tuning mechanism would be required for narrowband high-order filters. To this purpose, the inclusions of the tuning elements within the simulated and optimized 3-D EM model would guarantee the ability to compensate both positive and negative deviations from the nominal dimensions.

IV. Conclusion

In this letter, we introduced and validated an innovative structure based on direct-coupled TE–TM sections that can hopefully pave the way for the definition of a new class of nonresonating mode waveguide filters. Due to the size reduction provided by the quarter-wave long sections, as well as the order reduction derived from the introduction of transmission zeros, these new filters would be able to upgrade any system currently employing bulky waveguide filters (such as those employed below the X-band for SATCOM, communication, and radar applications). When considering the complex structure of a higher order filter where the offsets and angles of several sections must be accurately synthesized, the introduction of proper design techniques capable of offering a decently accurate first dimensioning of the structure appears to be a much-needed initial step to make these designs practical. Regarding the final 3-D EM optimization, besides mode-matching and integral equation modal simulation tools, other efficient numerical methods (such as the one proposed in [13]) could allow for the inclusion of potential tuning elements (as well as rounded internal edges for CNC machining) while guiding the optimization process due to the extraction of the actual coupling coefficients. Undoubtedly, the design and validation of higher order structures employing more than three sections is going to be the next step toward the definition of this new class of direct-coupled TE–TM waveguide filters.

References

[1] R. V. Snyder, G. Macchiarella, S. Bastioli, and C. Tomassoni, "Emerging trends in techniques and technology as applied to filter design," *IEEE J. Microw.*, vol. 1, no. 1, pp. 317–344, Jan. 2021.

[2] U. Rosenberg, S. Amari, and J. Bornemann, "Inline TM_{110}-mode filters with high design flexibility by utilizing bypass couplings of nonresonating $TE_{10/01}$ modes," in *IEEE Trans. Microw. Theory Tech.*, vol. 51, no. 6, pp. 1735–1742, Jun. 2003.

[3] M. Guglielmi, P. Jarry, E. Kerherve, O. Roquebrun, and D. Schmitt, "A new family of all-inductive dual-mode filters," *IEEE Trans. Microw. Theory Techn.*, vol. 49, no. 10, pp. 1764–1769, Oct. 2001.

[4] S. Bastioli, C. Tomassoni, and R. Sorrentino, "A new class of waveguide dual-mode filters using TM and nonresonating modes," *IEEE Trans. Microw. Theory Techn.*, vol. 58, no. 12, pp. 3909–3917, Dec. 2010.

[5] C. Tomassoni, S. Bastioli, and R. Sorrentino, "Generalized TM dual-mode cavity filters," *IEEE Trans. Microw. Theory Techn.*, vol. 59, no. 12, pp. 3338–3346, Dec. 2011.

[6] S. Bastioli and R. V. Snyder, "Stubbed waveguide cavity filters," *IEEE Trans. Microw. Theory Techn.*, vol. 67, no. 12, pp. 5049–5060, Dec. 2019.

[7] S. Bastioli and R. V. Snyder, "New triple-resonance configuration using stubbed waveguide dual-mode cavities," *IEEE Microw. Wireless Compon. Lett.*, vol. 32, no. 6, pp. 652–655, Jun. 2022.

[8] S. Bastioli and R. V. Snyder, "Nonresonating modes do it better! Exploiting additional modes in conjunction with operating modes to design better quality filters," *IEEE Microw. Mag.*, vol. 22, no. 1, pp. 20–45, Jan. 2021.

[9] U. Rosenberg, S. Amari, J. Bornemann, and R. Vahldieck, "Compact pseudo-highpass filters formed by cavity and iris resonators," in *Proc. 34th Eur. Microw. Conf.*, 2004, pp. 985–988.

[10] C. Bartlett, J. Bornemann, and M. Höft, "Improved TM dual-mode filters with reduced fabrication complexity," *IEEE J. Microw.*, vol. 3, no. 1, pp. 60–69, Jan. 2023.

[11] C. Bartlett, O. Glubokov, F. Kamrath, and M. Höft, "Highly selective broadband mm-wave diplexer design," *IEEE Microw. Wireless Technol. Lett.*, vol. 33, no. 2, pp. 149–152, Feb. 2023.

[12] J. F. V. Sullca, S. Cogollos, V. E. Boria, and M. Guglielmi, "Compact dual-band and wideband filters with resonant apertures in rectangular waveguide," *IEEE Trans. Microw. Theory Techn.*, vol. 70, no. 6, pp. 3125–3140, Jun. 2022.

[13] V. de la Rubia, "Description of microwave circuits via the reduced-basis method giving physical insight," *IEEE Trans. Antennas Propag.*, vol. 70, no. 11, pp. 10554–10568, Nov. 2022.